

# Grazing Bifurcations and Chaos of a Hydraulic Engine Mount

J.Marzbanrad\*, M.A.Babalooei

1Associated Professor, 2MSc. School of Automotive Engineering, Iran University of Science and Technology, Iran

\* Corresponding Author

## Abstract

The constitutive relationships of the rubber materials that act as the main spring of a hydraulic engine mount are nonlinear. In addition to material induced nonlinearity, further nonlinearities may be introduced by mount geometry, turbulent fluid behavior, temperature, boundary conditions, decoupler action, and hysteretic behavior. In this research all influence the behavior of the system only certain aspects are realistically considered using the lumped parameter approach employed. The nonlinearities that are readily modeled by the lumped parameter approach constitute the geometry and constitutive relationship induced nonlinearity, including hysteretic behavior, noting that these properties all make an appearance in the load-deflection relationship for the hydraulic mount and may be readily determined via experiment or finite element analysis. In this paper we will show that under certain conditions, the nonlinearities involved in the hydraulic mounts can show a chaotic response.

**Keywords:** Chaotic, Hydraulic engine mount, Inertia track, Decoupler

## Introduction

The automotive engine-chassis-body system may undergo undesirable vibration due to disturbances from the road and the engine. The engine vibration and road-induced vibration at idle are typically at frequencies below 50 Hz, while the engine oscillations vary from 50 to 200 Hz. Hydraulic engine mounts are effective passive vibration isolation devices used to isolate these two distinct modes of vibration (i.e., low-amplitude- high-frequency and high-amplitude-low-frequency) in automobiles. A typical hydraulic engine mount is designed to have high stiffness and damped response for low-frequency and large amplitude vibrations. In most cars, the engine vibration at 1 to 50 Hz is greater than 0.3 mm in amplitude. Conversely, at high-frequency, small amplitude vibrations, a hydraulic engine mount is designed for low stiffness, and damping characteristics (amplitudes less than 0.3 mm at 50-300 Hz).

This paper describes the modeling of a simple hydraulic engine mount as shown in Figure 1. At the

top, a hydraulic mount is in contact with the automotive engine, and in the bottom it is in contact with the chassis. The unit contains rubber components on top and bottom, two fluid chambers, an inertia track, and a decoupler.

The fluid in the hydraulic mount is normally water containing ethylene glycol. The engine vibration causes the rubber compliance structure on top to move up and down, thus forcing the fluid to travel between the upper and lower chambers through the decoupler and the inertia track. The decoupler in most designs, is an open cage containing a moving plate. As the fluid moves from one chamber to another, the decoupler plate moves in that direction until reaching the bottom or top constraints of the decoupler cage. The remaining flow is then forced mainly via the inertia track. The inertia track is a tube providing the engine mount with high damping at large excitation amplitudes. In this simple passive device, for small amplitude excitations, the fluid passes primarily through the decoupler with low resistance, and for large excitations the fluid is forced through the higher resistance inertia track. The lower chamber, like a balloon, is expanded or contracted due to the lower compliance rubber. The decoupler action is therefore

extremely important to tune the damping and frequency of the hydraulic mount and therefore to optimize its effectiveness to isolate vibrations. In many cases, the designs of these components are conducted through trial and error. A proper model of the decoupled would allow the designer to study the behavior of the hydraulic mount more effectively, and it would minimize the development time. This report provides a simple nonlinear model of the mount decoupled based on basic dynamic and fluid principles.

### 1. Simulation Model

The hydraulic engine mount equations may be obtained considering an ideal model shown in Figure-2. As the engine oscillates, it applies a force  $F(t)$  to the hydraulic mount. Also the engine displacement is defined by  $x(t)$ . The engine displacement pushes down the top rubber components, forcing the fluid in the top chamber to flow via the inertia track and the decoupler to the bottom chamber. Both chambers are idealized to have the same cross-sectional area  $A_p$ . The following transformation is used to relate the flow in the inertia track and the decoupler to the fluid velocity respectively:

Displacement in the inertia track and decoupler chambers.

The momentum equation can be noted with assuming the inertia track and the decoupler cross-sectional areas are  $A_i$  and  $A_d$ , respectively:

$$(P_1 - P_2)A_i = M_i \ddot{x}_i + F_i \quad (1)$$

$$(P_1 - P_2)A_d = M_d \ddot{x}_d + F_d + F(x_i, \dot{x}_d) \quad (2)$$

where the subscripts  $i$  and  $d$  correspond respectively to the inertia track and the decoupler.  $F(x_d, \dot{x}_d)$  is a nonlinear function depends on the function of the decoupler and shows the variation of its resistance due to displacement of its plate. The proposed function for the decoupler resistance is

$$F(x_d, \dot{x}_d) = E \frac{x_d^n}{\Delta^n} \dot{x}_d, \quad n = 2m, \quad m \in N \quad (3)$$

where  $E$  is a constant depending on the hydraulic mount geometry and must be obtained experimentally. The simplest representation of  $F(x_d, \dot{x}_d)$  is a cubic function which may be used for theoretical analysis.

$$F(x_d, \dot{x}_d) = E \frac{x_d^2}{\Delta^2} \dot{x}_d \quad (4)$$

$F_i$  and  $F_d$  are the fluid resistances depend on two parameters  $B_i$  and  $B_d$ , which are constants depending on fluid properties and geometric parameters of the corresponding flow channels. That is,

$$F_i = B_i \left( \frac{Q_i}{A_i} \right)^{\alpha_i}, \quad F_d = B_d \left( \frac{Q_d}{A_d} \right)^{\alpha_d} \quad (5)$$

where  $\alpha_i$  and  $\alpha_d$  define if the flow through the inertia track or decoupler is laminar or turbulent respectively. The mount continuity conditions are written as:

$$A_p \dot{x} - Q_d - Q_i = C_1 (\dot{P}_1 - \dot{P}_0)$$

$$Q_d + Q_i = C_2 (\dot{P}_2 - \dot{P}_0) \quad (6)$$

where  $P_0 = 0$  and  $C_1$  and  $C_2$  are the compliance (or the capacitance) associated with the upper and lower chambers, respectively. Differentiating (2) with respect to time, and using (1), (5), and (6), the internal hydraulic mount dynamics may be derived. The resulting flow equations are written as:

$$\begin{bmatrix} \frac{M_i}{A_i^2} & 0 \\ 0 & \frac{M_d}{A_d^2} \end{bmatrix} \begin{Bmatrix} \ddot{Q}_i \\ \ddot{Q}_d \end{Bmatrix} + \begin{bmatrix} \frac{B_i \alpha_i Q_i^{\alpha_i-1}}{A_i^{\alpha_i+1}} & 0 \\ 0 & \frac{B_d \alpha_d Q_d^{\alpha_d-1}}{A_d^{\alpha_d+1}} \end{bmatrix} \begin{Bmatrix} \dot{Q}_i \\ \dot{Q}_d \end{Bmatrix} + \begin{bmatrix} K & K \\ K & K \end{bmatrix} \begin{Bmatrix} Q_i \\ Q_d \end{Bmatrix} + \frac{F}{A_d} \begin{Bmatrix} 0 \\ 1 \end{Bmatrix} = \frac{A_p \dot{x}}{C_1} \begin{Bmatrix} 1 \\ 1 \end{Bmatrix} \quad (7)$$

where  $K = \frac{1}{C_1} + \frac{1}{C_2}$ .

In the case the flow through the inertia track and the decoupler is assumed to be laminar,  $\alpha_i$  and  $\alpha_d = 1$  and (5) becomes linear. That is,

$$\begin{bmatrix} M_i & 0 \\ 0 & M_d \end{bmatrix} \begin{Bmatrix} \ddot{x}_i \\ \ddot{x}_d \end{Bmatrix} + \begin{bmatrix} B_i & 0 \\ 0 & B_d \end{bmatrix} \begin{Bmatrix} \dot{x}_i \\ \dot{x}_d \end{Bmatrix} + \begin{bmatrix} A_i^2 K & A_i A_d K \\ A_i A_d K & A_d^2 K \end{bmatrix} \begin{Bmatrix} x_i \\ x_d \end{Bmatrix} + F(x_i, \dot{x}_d) \begin{Bmatrix} 0 \\ 1 \end{Bmatrix} = \frac{A_p \dot{x}}{C_1} \begin{Bmatrix} A_i \\ A_d \end{Bmatrix} \quad (8)$$

If the equation (8) be arranged and the equation (4) is used, the following nonlinear equations of motion are obtained:

$$\begin{bmatrix} 1 & 0 \\ 0 & 1 \end{bmatrix} \begin{Bmatrix} \ddot{x}_i \\ \ddot{x}_d \end{Bmatrix} + \begin{bmatrix} \frac{B_i}{M_i} & 0 \\ 0 & \frac{B_d}{M_d} + \frac{E}{M_d \Delta^2} x_d^2 \end{bmatrix} \begin{Bmatrix} \dot{x}_i \\ \dot{x}_d \end{Bmatrix} + \begin{bmatrix} \frac{A_i^2 K}{M_i} & \frac{A_i A_d K}{M_i} \\ \frac{A_i A_d K}{M_d} & \frac{A_d^2 K}{M_d} \end{bmatrix} \begin{Bmatrix} x_i \\ x_d \end{Bmatrix} = \frac{A_p \dot{x}}{C_1} \begin{Bmatrix} \frac{A_i}{M_i} \\ \frac{A_d}{M_d} \end{Bmatrix} \quad (9)$$

By using the following no dimensional parameters,

$$\tau = \Omega t, \Omega^2 = \frac{A_d^2 K}{M_d}, x_d = \Delta y_d, x_i = \Delta y_i, x = \Delta y \quad (10)$$

the equations of motion (9) become

$$\begin{bmatrix} 1 & 0 \\ 0 & 1 \end{bmatrix} \begin{Bmatrix} \ddot{y}_i \\ \ddot{y}_d \end{Bmatrix} + \begin{bmatrix} \frac{B_i}{M_i \Omega} & 0 \\ 0 & \frac{B_d + E y_d^2}{M_d \Omega} \end{bmatrix} \begin{Bmatrix} \dot{y}_i \\ \dot{y}_d \end{Bmatrix} + \begin{bmatrix} \frac{A_i^2 M_d}{M_i A_d^2} & \frac{A_i M_d}{M_i A_d} \\ \frac{A_i}{A_d} & 1 \end{bmatrix} \begin{Bmatrix} y_i \\ y_d \end{Bmatrix} = \frac{A_p Y}{C_1 A_d K} \begin{Bmatrix} \frac{A_i M_d}{M_i A_d} \\ 1 \end{Bmatrix} \quad (11)$$

For the non-linearity of the differential equations the state variables and the equations of motion is assumed:

$$\begin{aligned} y &= (x_i, v_i, x_d, v_d)^T; \\ \dot{x}_i &= v_i \\ \dot{v}_i &= -\left(\frac{B_i}{M_i \times \Omega}\right) \times v_i - \left(\frac{A_i^2 \times M_d}{M_i \times A_d^2}\right) \times x_i - \\ &\quad \left(\frac{A_i \times M_d}{M_i \times A_d}\right) x_d + \left(\frac{A_p \times A_i \times M_d}{C_1 \times A_d^2 \times K \times M_i}\right) \times Y \times \sin(\omega \times t) \\ \dot{x}_d &= v_d \\ \dot{v}_d &= -\left(\frac{B_d + E \times x_d^2}{M_d \times \Omega}\right) \times v_d - \left(\frac{A_i}{A_d}\right) \times x_i - x_d + \\ &\quad \left(\frac{A_p}{C_1 \times A_d \times K}\right) \times Y \times \sin(\omega \times t) \end{aligned} \quad (12)$$

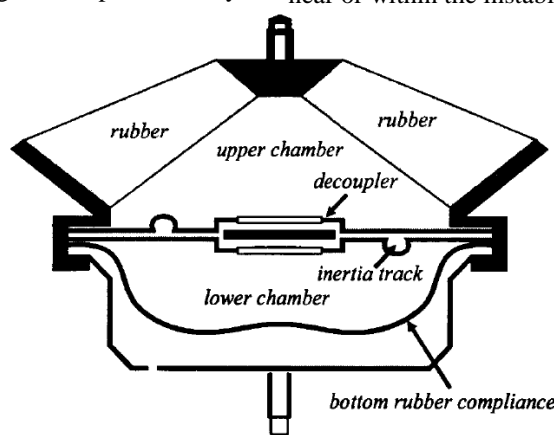
### 3. Numerical Results

Owing to the non-linearity of the differential equations (12), the dynamic response of the hydraulic engine mount model was studied numerically with the fourth order Runge–Kutta algorithm provided by

MATLAB. The absolute error tolerance, in the computation, was less than  $10^{-6}$ . Since numerical integration could give spurious results with regard to the existence of chaotic due to insufficiently small time steps, the step size was verified to ensure no such results were generated as a result of time discretization. The mount parameter set assumed for the numerical study is shown in Table 1.

It is known that the dynamics of a system may be analyzed via a frequency-response diagram, which is obtained by plotting the amplitude of the oscillating system versus the frequency of the excitation term [11, 12]. For the mount system, the frequency-response diagram was calculated numerically. For the inertia track and decoupler, the amplitude was defined as the maximum absolute value of the displacement and the control parameter was defined as the forcing frequency of the excitation from engine respectively.

Fig. 3 represents one of the frequency-response diagrams of the model when the forcing frequency  $f$  is slowly increased. The amplitude of the forcing function  $Y = 0.1$  mm. The diagrams were calculated by using an increment  $\Delta\omega = 0.1$  Hz as the variation of the control parameter. As illustrated in Figs. 3(a) the first jump is observed at  $\omega = 70$  Hz; then the second jump is at  $\omega = 120$  Hz; then the third jump is at  $\omega = 155$  Hz as forcing frequency increased. The phenomenon of the three jumps can also be observed in response diagram of the decoupler of hydraulic engine mount shown in Fig. 3(b). However, the diagram exhibits a more complicated and different behavior. This is confirmed by the presence of more jumps in this diagram as the forcing frequency increased. Fig. 3. shows that the responses of the system have instability region as  $60 < \omega < 125$  Hz and  $143 < \omega < 200$  Hz; which indicates that the chaotic responses are possible when the forcing frequency is near or within the instable region [13–15].



Cross-section of the hydraulic mount

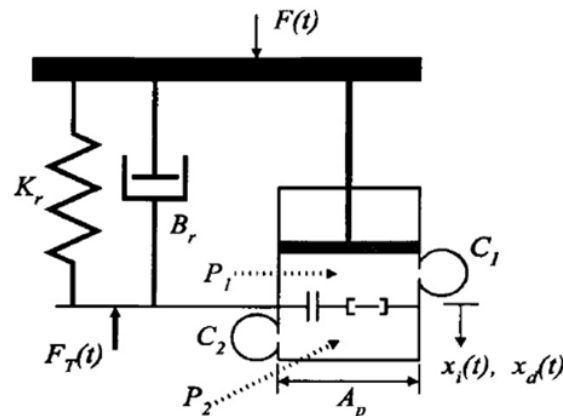


Fig1.A lumped parameter fluid system model of the hydraulic engine mount.

Table 1. Parameters for numerical simulation [21]

$A_p$	$5.027\text{e-}3\text{ [m}^2\text{]}$
$A_i$	$5.72\text{e-}5\text{ [m}^2\text{]}$
$A_d$	$2.3\text{e-}3\text{ [m}^2\text{]}$
$M_i$	$0.37\text{e-}2\text{ [kg]}$
$M_d$	$2.645\text{e-}2\text{ [kg]}$
$E$	$2.9095$
$B_i$	$4.83\text{e-}3\text{ [N.s/m]}$
$B_d$	$2.9\text{ [N.s/m]}$
$C_1$	$4.6\text{e-}10\text{ [m}^5\text{/N]}$
$C_2$	$4.6\text{e-}8\text{ [m}^5\text{/N]}$

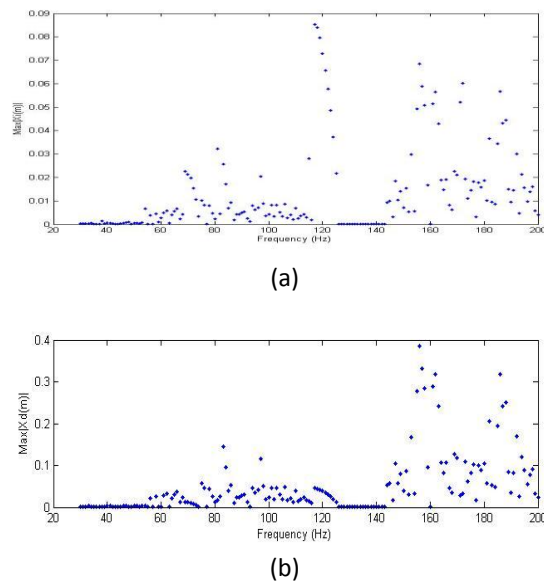


Fig2.Frequency-response diagrams when the forcing frequency f is slowly increased (Y =0.1 mm): (a) Inertia track (b) Decoupler

The bifurcation diagram is a widely used technique for examining the changes of responses in a dynamic system under parameter variations. To make the bifurcation diagram, some measure of the motion is plotted as a function of the system parameter.

As shown in Fig. 4, the bifurcation diagram is obtained by plotting the Poincare points of the inertia track displacement  $X_i(t)$  against the amplitude of harmonic engine excitation  $\omega$ . The amplitude of harmonic engine excitation used in the computation were  $\omega = 100$  Hz. In this diagram, amplitude varied from 0 to 0.3 mm according to 1500 equal steps. For every parameter amplitude; the responses of the system from 0 to 400 s that was 1440 forcing cycles, were computed. To eliminate the transient responses, only the last 150 points of the Poincare section associated with the 150 last periods were saved. The initial conditions were set  $[0,0,0,0]$  for every

parameter. The different behavior was observed as the values of amplitude were in the range of 0–0.3 mm. In Fig. 4, the responses of the system could become chaotic very quickly as the amplitude is around 0.21 mm. This implies that the periodic responses of the model may jump to chaotic one even there is only a small change in amplitude of harmonic engine excitation.

Fig. 5 represents the bifurcation of  $X_d(t)$  by varying the values of the parameter amplitude from 0 to 0.3mm according to 1500 equal steps. The time span for the computation was from 0 to 400 s and The initial condition was set to  $[0,0,0,0]$ . As the computation for Fig. 4, the last 150 Poincare points were preserved for plotting the diagram. The enlargements of the diagram in Fig. 5 are shown in Figs. 6. These bifurcation diagrams exhibit period windows and crisis as the time delay amplitude is around  $0.18 < Y < 0.3$  mm.

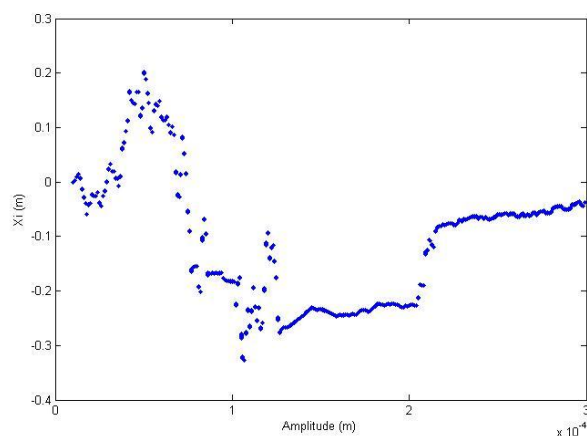
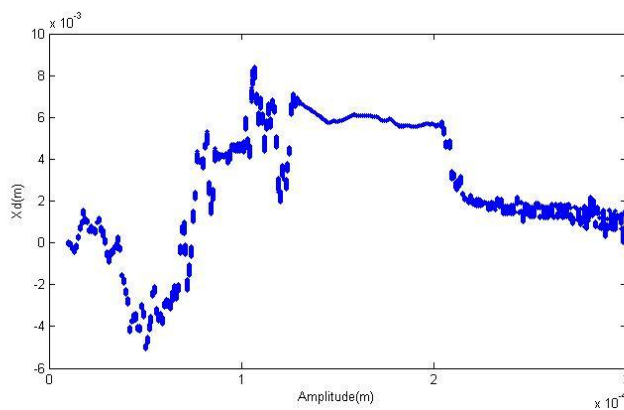


**Fig3.** The bifurcation diagram of the inertia track



The bifurcation diagram of decoupler

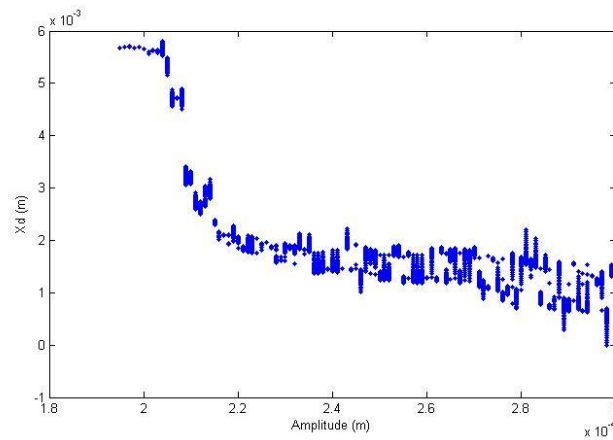


**Fig4.** Enlargements of the bifurcation diagram of Fig. 3.

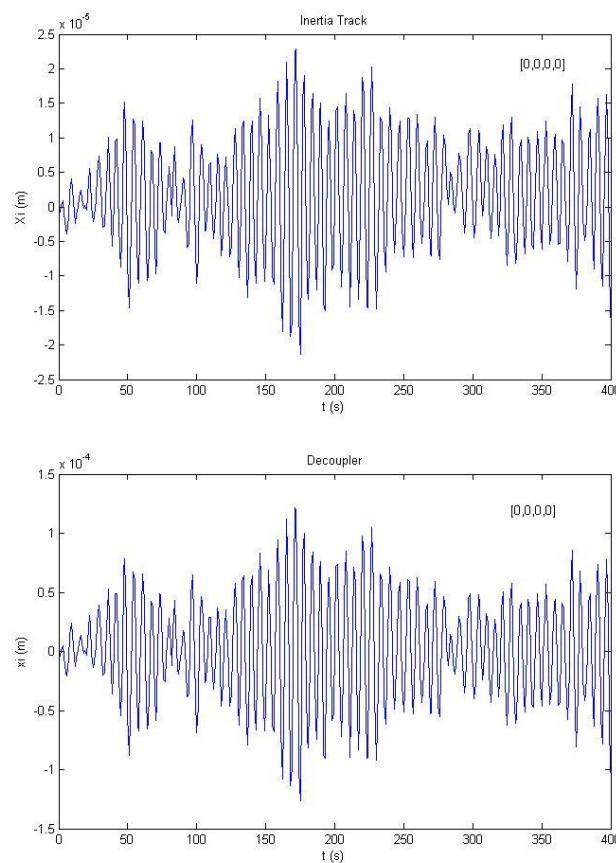


**Fig5.** Time histories of chaotic motion of the system ( $Y = 0.03$  mm;  $\omega = 100$  Hz; the remaining parameters are shown in Table 1).



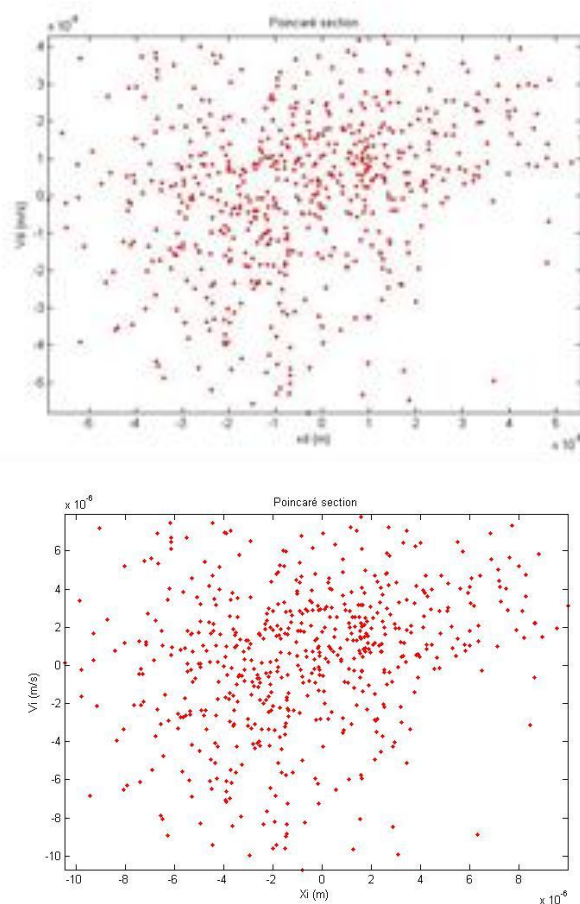


**Fig6.** Poincaré maps of chaotic motion of the system ( $Y=0.01$  mm;  $\omega = 100$  Hz).

### Conclusion

The chaotic responses and bifurcations of a hydraulic engine mount model are studied through numerical simulation. It is found that the chaotic response may exist in the instable region of frequency-response diagram. The bifurcation diagram shows that the chaotic response could be sensitive to variation of amplitude of the harmonic engine excitation. Although the mechanical model of the hydraulic engine mount is only a simplified one and the parameters used do not agree closely with the practical data for an automobile, the results may still be useful in dynamic design of the ground vehicle. The confirmation of the existence of the chaos in this kind of model by experiment is left for further study.

One of the time histories of  $X_i(t)$  and  $X_d(t)$  are plotted in Fig. 7. The time history data of the first 1700 forcing cycles were not used in order to guarantee that the data used were in a steady state.

The Poincaré maps of the responses of the engine mount corresponding to time histories in Fig. 7 are shown in Fig. 8. Each Poincaré map contains 4200 sampling points. Fig. 8 shows the existence strange attractors. These results indicated that the responses of the system of hydraulic engine mount were chaotic.

## References

- [1]. S. Strogatz, *Nonlinear dynamics and Chaos*, Addison-Wesley, New York, 1994.
- [2]. H. G. Schuster, *Deterministic Chaos: An Introduction*, VCH, Weinheim, Germany, 1988.
- [3]. R. M. Brach and A. Haddow, on the dynamic response of hydraulic engine mounts, SAE Technical Paper Series 931321 (1993).
- [4]. A. Geisberger, A. Khajepour and F. Golnaraghi, Non-linear Modeling of Hydraulic Engine Mounts: Theory and Experiment, *Journal of Sound and Vibration* (2002).
- [5]. G. P. Williams, *Chaos theory tamed*, Joseph Henry Press, 1997.
- [6]. A. Fidlin, *Nonlinear oscillations in mechanical engineering*, Springer, 2005.
- [7]. A. Stensson, C. Asplund, and L. Karlsson, The nonlinear behaviour of a MacPherson strut wheel suspension, *Vehicle System Dynamics*, vol. 23, pp. 85-106, 1994.
- [8]. F. C. Moon, *Chaotic and fractal dynamics*, John Wiley & Sons Inc, 1992.
- [9]. G. L. Baker, *Chaotic dynamics: an introduction*, Cambridge University Press, 1996.
- [10]. H. G. Schuster and W. Just, in *Deterministic Chaos: An introduction*, ed: Wiley-VCH Verlag GmbH & Co. KGaA, 2005, pp. i-xi.
- [11]. S. Strogatz, *Nonlinear dynamics and chaos: with applications to physics, biology, chemistry, and engineering (studies in nonlinearity)*, Perseus Books Group, 1994.
- [12]. D. H. Rothman, *Nonlinear Dynamics I: Chaos*, fall, 2005.
- [13]. j. Rimple, H. Stoll, J. Betzler, *The Automotive Chassis*, Butterworth-Heinemann, ISBN 07506 50540, 2001.
- [14]. H.K. Chen, Global chaos synchronization of new chaotic systems via nonlinear control, *Chaos Solitons & Fractals*, Vol. 23, pp. 1245-1251, 2005.
- [15]. L. P' ust, O. Sz. oll. os, The forced chaotic and irregular oscillations of the nonlinear two degrees of freedom (2dof) system, *International Journal of Bifurcation and Chaos* 9 (1999) 479-491.
- [16]. S. Grossmann, and S. Thomae, Invariant Distributions and Stationary Correlation Functions of One-Dimensional Discrete Processes, *Z. Naturforsch.* 32 A, 1353, 1977.
- [17]. A. Wolf, Simplicity and universality in the transition to chaos, *Nature* 305, 182-3, 1983.
- [18]. C. Grebogi, E. Ott, J. A. Yorke, Chaotic attractors in crisis, *Physical Review Letters* 48(22), 1507-510, 1982.
- [19]. A. Wolf, Quantifying chaos with Lyapunov exponents, In *Chaos*, A. V. Holden (ed.), 273-90. Princeton, New Jersey: Princeton University Press., 1986.
- [20]. C. F. Barengi, *Introduction to chaos: theoretical and numerical methods*, 2010.
- [21]. F. Golnaraghi and R. Nakhaie, Development and Analysis of A Simplified Nonlinear Model of A Hydraulic Engine Mount, *Journal of Vibration and Control* (2000).
- [22]. H. Adiguna, M. Tiwari, R. Singh and D. Hovat, Transient Response of a Hydraulic Engine Mount, *Journal of Sound and Vibration* (2003).
- [23]. W. B. Shangguan and Z. H. Lu, Modelling of a hydraulic engine mount with fluid-structure interaction finite element analysis, *Journal of Sound and Vibration* 2004.
- [24]. J. J. E Slotine, and W. Li, *Applied Nonlinear Control*, Englewood Cliffs, New Jersey: Prentice Hall (1991).
- [25]. R.A. DeCarlo, S.H. Zak and G.P. Matthews, Variable Structure Control of Nonlinear Multivariable System: A Tutorial, *Proceedings of the IEEE*, 76(3): 212-232, 1988.
- [26]. Q. Ming, *Sliding Mode Controller Design for ABS System*, Virginia Polytechnic Institute and State University: Master Thesis, 1997.
- [27]. G. Bartolini, and E. Punta, Second Order Sliding Mode Tracking2 Control of Underwater Vehicles, *Proceedings of the American Control3 Conference*, Chicago, Illinois, June 2000, ISBN 0-7803-5519-9
- [28]. C. Ünsal, and K. Kachroo, Sliding Mode Measurement Feedback4 Control for Antilock Braking Systems, *IEEE Transactions on control systems5 technology*, Vol. 7, no 2, 1999, ISSN 1063-6536
- [29]. S. Drakunov, U. Ozguner, P. Dix and B. Ashrafi, ABS Control using Optimum Search via Sliding Modes, *IEEE Transactions on Control Systems Technology*, 1995, 3(1):79-85.
- [30]. R. Singh, G. Kim and P. V. Ravindra, Linear Analysis of Automotive Hydro-Mechanical Mount with Emphasis on Decoupler Characteristics, *Journal of Sound and Vibration*, 158(2), 1992. pp. 219-243.
- [31]. Y. Yu, S. M. Peelamedu, N. G. Naganathan, R. V. Dukkipati, Automotive Vehicle Engine Mounting Systems: A Survey, *Journal of Dynamic Systems, Measurement, and Control*, Vol. 123, pp. 186-194, 2001.
- [32]. G. N. Jazar, F. Golnaraghi, Engine Mounts for Automotive Applications: A Survey, the *Shock and Vibration Digest*, Vol. 34, No. 5, pp. 363-379, 2002.
- [33]. N. Vahdati, Double-notch single-pumper fluid mounts, *Journal of Sound and Vibration*, Vol. 285, No. 3, pp. 697-710, and 2005.
- [34]. J. Christopherson, G. N. Jazar, Dynamic behavior comparison of passive hydraulic engine mounts, Part 2: Finite element analysis, *Journal of Sound and Vibration*, Vol. 290, No. 3, pp. 1071-1090, 2006.
- [35]. G. Kim, R. Singh, Nonlinear Analysis of Automotive Hydraulic Engine Mount, *Journal of Dynamic Systems Measurement and Control-*

Created with



nitro PDF<sup>®</sup>  
professional

download the free trial online at [nitropdf.com/professional](http://nitropdf.com/professional)



- Transactions of the Asme, Vol. 115, No. 3, pp. 482-487, 1993.
- [36]. M. R. Jolly, J. W. Bender, J. D. Carlson, Properties and applications of commercial magnetorheological fluids, *Journal of Intelligent Material Systems and Structures*, Vol. 10, No. 1, pp. 5-13, 1999.
- [37]. M. Ahmadian, Y. K. Ahn, Performance Analysis of Magneto-Rheological Mounts, *Journal of Intelligent Material Systems and Structures*, Vol. 10, No. 3, pp. 248-256, 1999.
- [38]. S. B. Choi, H. H. Lee, H. J. Song, J. S. Park, Vibration Control of a Passenger Car Using MR Engine Mounts, *Smart Structures and Materials*, Vol. Proceedings of SPIE Vol. 4701, 2002.
- [39]. M. Brigley, Y. T. Choi, N. M. Wereley, S. B. Choi, Magnetorheological Isolators Using Multiple Fluid Modes, *Journal of Intelligent Material Systems and Structures*, Vol. 18, pp. 1143-1148, 2007.
- [40]. S. Arzanpour, M. F. Golnaraghi, A Novel Semi-active Magnetorheological Bushing Design for Variable Displacement Engines, *Journal of Intelligent Material Systems and Structures*, Vol. 19, pp. 989-1003, 2008.
- [41]. D. E. Barber, J. D. Carlson, Performance characteristics of prototype MR engine mounts containing glycol MRfluids, *Journal of Intelligent Material Systems and Structures*, Vol. 21, No. 15, pp. 1509-1516, and 2010.
- [42]. A. K. Samantaray, and Amalendu, Bond graph in modeling, simulation and fault identification, IK International Pvt Ltd, 2006
- [43]. J. D. Carlson, D. M. Catanzarite, K. A. S. Clair, Commercial magnetorheological fluid devices, *International Journal of Modern Physics B*, Vol. 10, pp. 2857-2865, 1996.